Hindawi
Mathematical Problems in Engineering
Volume 2022, Article ID 9977188, 19 pages
https://doi.org/10.1155/2022/9977188

Research Article

An Exact and Comparative Analysis of MHD Free Convection Flow of Water-Based Nanoparticles via CF Derivative

Aziz-Ur- Rehman,[1] **Muhammad Bilal Riaz**,[1,2] **Syed Tauseef Saeed**,[3] **Fahd Jarad**,[4,5] **Hayder Natiq Jasim**,[6] **and Aytekin Enver**[7]

[1]*Department of Mathematics, University of Management and Technology Lahore, Lahore, Pakistan*
[2]*Institute for Groundwater Studies (IGS), University of the Free State, Bloemfontein, South Africa*
[3]*Department of Science & Humanities, National University of Computer and Emerging Sciences, Lahore Campus, Lahore, Pakistan*
[4]*Department of Mathematics, Çankaya University, Ankara, Turkey*
[5]*Department of Medical Research, China Medical University Hospital, China Medical University, Taichung, Taiwan*
[6]*Faculty of Science for Women, Baghdad University, Baghdad, Iraq*
[7]*Department of Mathematics, Gazi University, Teknikokullar, Ankara, Turkey*

Correspondence should be addressed to Fahd Jarad; fahd@cankaya.edu.tr

Received 13 March 2021; Revised 17 September 2021; Accepted 24 March 2022; Published 16 June 2022

Academic Editor: Parviz Ghadimi

Convective flow is a self-sustained flow with the effect of the temperature gradient. The density is nonuniform due to the variation in temperature. The effect of the magnetic flux plays a major role in convective flow. The process of heat transfer is accompanied by a mass transfer process, for instance, condensation, evaporation, and chemical process. Combination of water as base fluid and three types of nanoparticles named as copper, titanium dioxide, and aluminum oxide is taken into account. Due to the applications of the heat and mass transfer combined effects in different fields, the main aim of this paper is to do a comprehensive analysis of heat and mass transfer of MHD natural convection flow of water-based nano-particles in the presence of ramped conditions with Caputo–Fabrizio fractional time derivative. The exact fractional solutions of temperature, concentration, and velocity have been investigated by means of integral transform. The classical calculus is assumed as the instant rate of change of the output when the input level changes. Therefore, it is not able to include the previous state of the system called the memory effect. But, in the fractional calculus (FC), the rate of change is affected by all points of the considered interval to incorporate the previous history/memory effects of any system. Due to this reason, we applied the modern definition of fractional derivative. Here, the order of the fractional derivatives will be treated as an index of memory. The influence of physical parameters and flow is analyzed graphically via computational software (MATHCAD-15). Our results suggest that the incremental value of the M is observed for a decrease in the velocity field, which reflects to control resistive force.

1. Introduction

Convective flow is a self-sustained flow that transfers heat energy into or out of the body by actual movement of fluids particles that move energy with its mass. Thermal radiation and the effect of magnetic flux play an important role in convective flow. The different industrial problems and fluid flow in the porous medium have achieved consideration in recent years. In the literature, different theories are made to see the phenomenon of heat and mass transfer analysis. Radiation, convection, and conduction are three modes of heat transfer. Convection can be defined as heat transfer by the substance motion which may be air or water. It plays a central role in creating the weather clause on the plant. Nanoliquids are used to enhance the thermo-physical properties and the performance of conventional fluids in cooling and heating methods such as decrease the power of nuclear reactors, reduce temperature in vehicles radiators,

controlled heat in different computer progressions, and handling thermal flows. In pharmaceutical industry, diagnoses and treatment of cancer are based on nanoliquid operators which comprise of different radiations. These noteworthy physical attributes of nanofluids and their implications are fascinating scientists and researchers. The term nanofluid is referred to the addition of some solid nanoparticles in regular fluid, sometimes known as base fluid. This idea was first introduced by Choi [1]. Nano-sized particles are used to raise the thermal conductivity of traditional fluids such as water and mineral oils. The creation of nanometer-sized particles involves carbides, carbon nanotubes, and metals. Nanocompounds have substantial applications in several procedures such as drugs delivery, water purification, bio diesel invention, and creation of carbon nanotubes, according to Sarli et al. [2]. Masuda et al. [3] presented higher thermo physical properties in nanofluids due to some nanosized particles, undoubtedly, huge difference in the structure of nanoparticles because it has different shape and size. Das et al. [4] studied that for different temperature range between 200 C to 500 C, the thermal conductivities of TiO_2 and Al_2O_3 water-base fluids increased at most four times.

The study of mass and thermal flows of incompressible, viscous nanofluids is highly significant because of essential applications of such flows in engineering, chemistry, and physics. Imposition of external magnetic field and placement of cavities filled with fluid and porous medium affect the flow of electrically insulated fluid in bearings, pumps, MHD motors, and generators. Such cavities can be portioned as horizontal and vertical cavities. Hamad et al. [5] observed the characteristics of fluid flow containing nanometer-sized particles over a vertical plate in the presence of the external magnetical field. The impacts of magnetic strength on some nanofluid flow are investigated by Das and Jana [6]. Turkyilmazoglu [7] discussed the mass with heat transmission of exact investigation of MHD flow of some fluids having nanometer-sized particles. The movement of nanofluid on a porous surface placement in a revolving system is examined by Sheikholeslami and Ganji [8]. Husanan et al. [9] presented the unsteady movement of nanofluids nested in a porous medium in the existence of an electromagnetic field. In [10–12], researchers studied and discussed the influence of exothermically and radiating heat for some microlevel fluid flow. Khan et al. [13] studied Casson-type nanofluid movement in the occurrence of thermo-radiation and heat consumption. In [14–18], some identical studies can be investigated. Ahmed and Dutta [19] first time floated the idea of effective velocity and temperature with ramped wall conditions at a similar time for mass transmission of Newtonian unsteady fluid flow transient through impulsively affecting long vertical plate. Generally, ramped velocity has a great advantage in the medical field especially diagnosed, and treatment for heart, blood, and cancer diseases is discussed and studied in [20–22]. Schetz [23], Hayday [24], and Malhotra et al. [25] are investigated nonuniform and time-dependent temperatures with ramped conditions. Kundu [26] highlighted important operability time-dependent conditions for temperature and also suggested five different forms of heating. Keolyar et al. [27] observed controlled heat conditions on unstable MHD radiated movement of some fluids with nanoparticle mixtures passing through a flat surface plate. Some researchers have discussed noteworthy facts of heat emission and mass transfer and elaborated under dissimilar physical phenomena in [28–30].

The technique of fractional calculus has been used to formulate mathematical modeling in various technological development, engineering applications, and industrial sciences. Different valuable work has been discussed for modeling fluid dynamics, signal processing, viscoelasticity, electrochemistry, and biological structure through fractional time derivatives [31–33]. This fractional differential operator found useful conclusions for experts to treat cancer cells with a suitable amount of heat source and have compared the results to see the memory effect of temperature function. As compared to classical models, the memory effect is much stronger in fractional derivatives [34–39]. Over the last thirty years, fractional derivative/calculus (FDs/FC) has captivated numerous researchers after recognition of the fact that in comparison to the classical derivatives, FDs are more reliable operators to model real-world physical phenomena. In dynamical problems, fractional-order model/modeling is receiving rapid popularity nowadays. The mathematical modeling of many physical and engineering models based on the idea of FC exhibits highly precise and accurate experimental results as compared to the models based on conventional calculus. For example, the fractional results of rate and differential type fluids have a great resemblance with the results obtained experimentally. For nonsingular kernel convective flow with ramped conditions, the temperature is studied by Riaz et al. [40]. Furthermore, the same author Riaz et al. [41] highlighted the heat effect on MHD Maxwell fluid by using local and nonlocal operators. Some other associated references dealing with fractional differential operators, MHD Maxwell fluid movement, heat emission, or fractional second-grade fluid are given in [42–54].

Recently, Talha Anwar et al. [55] studied MHD-free convective flow of water base nanofluids having three types of nanoparticles named copper, titanium dioxide, and aluminum oxide [56], with the classical approach. They have not analyzed the behavior of fractional derivatives. The intent of this manuscript is to explore the exact and closed-form solution of MHD-free convective flow of water base nanofluids with the Caputo–Fabrizio fractional operator with simultaneous use of ramped heating with ramped velocity. Laplace integral transformation is used to gain the solutions of velocity, temperature, and concentration under the impact of ramped conditions. In Section 2, the dimensionless governing equations are developed. In Section 3, a noninteger order derivative with Laplace integral transform is used to find the required solution of the concentration, temperature, and velocity field. In Section 4, the effect of physical parameters is analyzed graphically. The concluding observation is listed at the end.

2. Mathematical Model

Let us assume that incompressible unsteady-free convective MHD fluid movement through a vertical plate is nested in a porous material with ramped temperature and energy transmission of a nanofluid. Both the fluid and plate have temperature T_∞, concentration C_∞ at initial time $\tau = 0$. At $\tau > 0$, motion is started in the plate with velocity $U_0\tau/\tau_0$, also temperature raised to $T_\infty + (T_w - T_\infty)\tau/\tau_0$ in the long vertical plate for $0 < \tau \le \tau_0$. But, later on, the plate maintained constant temperature T_w, concentration C_w, and moving with uniform velocity U_0 for $\tau > \tau_0$. Suppose that the fluid flow is unidirectional and one dimensional with x-axis is assumed along the vertical plate, y-axis is considered in perpendicular direction to the plate, and plate is placed at $y = 0$ but nanofluid movement to be constrained for $y > 0$. Figure 1 provided the geometrical and physical interpretation of the considered model. Also, nanofluid is contained water as a base fluid and Cu, TiO_2 and Al_2O_3 as nanoparticles. In the light of all aforementioned assumptions, the principal governing equations for a nanofluid can be expressed subject to the Boussinesq's approximation are given as [19, 46, 55]

$$\begin{aligned}
\rho_{nf}\frac{\partial u(y,\tau)}{\partial \tau} &= \mu_{nf}\frac{\partial^2 u(y,\tau)}{\partial y^2} + \frac{\mu_{nf}\gamma_2}{k^*}u(y,\tau) + g(\rho\beta_T)_{nf}(T(y,\tau) - T_\infty) \\
&\quad + g(\rho\beta_C)_{nf}(C(y,\tau) - C_\infty) - \sigma_{nf}\beta_0^2 u(y,\tau), \\
(\rho C_p)_{nf}\frac{\partial T(y,\tau)}{\partial \tau} &= \left(K_{nf} + \frac{16\sigma_r T_\infty^3}{3k_r}\right)\frac{\partial^2 T(y,\tau)}{\partial y^2} - Q_0 T(y,\tau) + Q_0 T_\infty, \\
\frac{\partial C(y,\tau)}{\partial \tau} &= D_{nf}\frac{\partial^2 C(y,\tau)}{\partial \tau^2}.
\end{aligned} \tag{1}$$

The corresponding initial and boundary conditions are stated as

$$u(y,0) = 0, T(y,0) = T_\infty, C(y,0) = C_\infty, \quad y \ge 0. \tag{2}$$

$$u(0,\tau) = f_1(\tau), T(0,\tau) = f_2(\tau), C(0,\tau) = C_w. \tag{3}$$

$$\begin{aligned}
f_1(\tau) &= \begin{cases} U_0\dfrac{\tau}{\tau_0}, & 0 < \tau \le \tau_0; \\ U_0, & \tau > \tau_0, \end{cases} \\
f_2(\tau) &= \begin{cases} T_\infty + (T_w - T_\infty)\dfrac{\tau}{\tau_0}, & 0 < \tau \le \tau_0; \\ T_w, & \tau > \tau_0. \end{cases}
\end{aligned} \tag{4}$$

$$\begin{aligned}
u(y,\tau) \longrightarrow 0, T(y,\tau) \longrightarrow \infty, C(y,\tau) \\
\longrightarrow \infty \text{ as } y \longrightarrow \infty.
\end{aligned} \tag{5}$$

The expressions for different properties of nanofluids then conventional fluids are density, specific heat capacity, coefficient of thermal expansion, electrical conductivity, thermal diffusion coefficient and dynamic viscosity are denoted by ρ_{nf}, $(\rho C_p)_{nf}$, $(\rho\beta)_{nf}$, σ_{nf}, D_{nf}, and μ_{nf} respectively and defined as

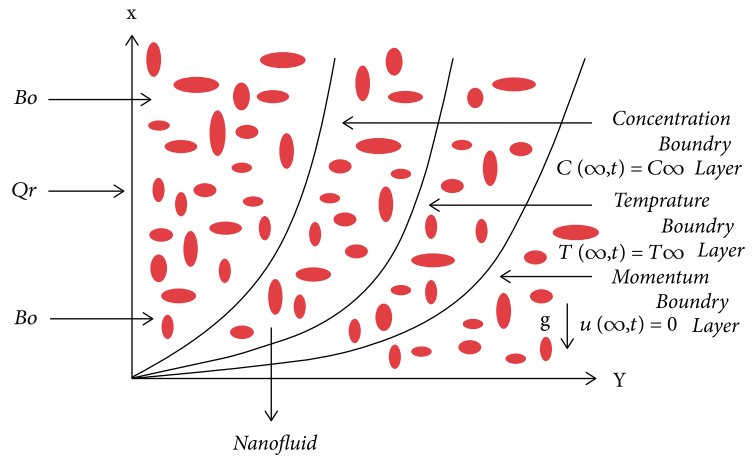

Figure 1: Geometrical presentation of the stated problem.

$$\mu_{nf} = \frac{\mu_w}{(1-\phi)^{2.5}}, \rho_{nf} = \rho_w\left(1-\phi+\phi\frac{\rho_{nf}}{\rho_w}\right), \sigma_{nf} = \sigma_w\left(1+\frac{3\phi(\sigma-1)}{(\sigma+2)-\phi(\sigma-1)}\right), \sigma = \frac{\sigma_{nf}}{\sigma_w},$$
$$\left(\rho C_p\right)_{nf} = \left(\rho C_p\right)_w\left(1-\phi+\phi\frac{\left(\rho C_p\right)_{nf}}{\left(\rho C_p\right)_w}\right), D_{nf} = (1-\phi)D_f, (\rho\beta)_{nf} = (\rho\beta)_w\left(1-\phi+\phi\frac{(\rho\beta)_{nf}}{(\rho\beta)_w}\right). \tag{6}$$

Also, the effective role of thermal conductivity for nanoparticles is discussed as

$$\frac{K_{nf}}{K_w} = \frac{K_{np}+2K_w-2\left(K_w-K_{nf}\right)\phi}{K_{np}+2K_w-\left(K_w-K_{nf}\right)\phi}. \tag{7}$$

Subscripts used in the above equations are w, nf, and np which are represented as base fluid, nanofluid, and nanoparticles, respectively. For nondimensionalization, we considered the following set of new variables:

$$\zeta = \frac{U_0}{v_w}y, \tau^* = \frac{U_0^2}{v_w}\tau, u^* = \frac{u}{u_0}, T^* = \frac{T-T_\infty}{T_w-T_\infty}, G_r = \frac{g(T_w-T_\infty)(v\beta_T)_w}{U_0^3},$$
$$C^* = \frac{C-C_\infty}{C_w-C_\infty}, G_m = \frac{g(C-C_\infty)(v\beta_c)_w}{U_0}, M = \frac{\sigma_w\beta_0^2 v_w}{\rho U_0^2}, N_r = \frac{16\sigma_r T_\infty^3}{3k_w k_r}, \tag{8}$$
$$P_r = \frac{\left(\mu C_p\right)_w}{k_w}, \frac{1}{K} = \frac{v_w^2\gamma_2}{k^* u_0^2}, Sc = \frac{v}{D_f}, Q = \frac{Q_0}{U_0^2}\left(\frac{v}{\rho C_p}\right)_w.$$

After employing the dimensionless quantities and removing the star notation, the following partial differential equations in the dimensionless form are derived as

$$\pi_1\frac{\partial u(\zeta,\tau)}{\partial\tau} = \pi_4\frac{\partial^2 u(\zeta,\tau)}{\partial\zeta^2} + \pi_2 G_r T(\zeta,\tau) + \pi_7 G_m T(\zeta,\tau) - \pi_3 M u(\zeta,\tau) - \pi_4\frac{u(\zeta,\tau)}{K}, \tag{9}$$

$$\frac{\partial T(\zeta,\tau)}{\partial\tau} = \left(\frac{\pi_5+N_r}{\pi_6 P_r}\right)\frac{\partial^2 T(\zeta,\tau)}{\partial\zeta^2} - \frac{Q}{\pi_6}T(\zeta,\tau), \tag{10}$$

$$\frac{\partial C(\zeta,\tau)}{\partial \tau} = b\frac{\partial^2 C(\zeta,\tau)}{\partial \zeta^2}, \tag{11}$$

where

$$\pi_1 = \left(1-\phi+\phi\frac{\rho_{nf}}{\rho_w}\right), \pi_2 = \left(1-\phi+\phi\frac{(\rho\beta_T)_{nf}}{(\rho\beta_T)_w}\right), \pi_3 = \left(1+\frac{3\phi(\sigma-1)}{(\sigma+2)-\phi(\sigma-1)}\right), \pi_4 = \frac{1}{(1-\phi)^{2.5}},$$
$$\pi_5 = \frac{K_{np}+2K_w-2\left(K_w-K_{nf}\right)\phi}{K_{np}+2K_w-\left(K_w-K_{nf}\right)\phi}, \pi_6 = \left(1-\phi+\phi\frac{\left(\rho C_p\right)_{nf}}{\left(\rho C_p\right)_w}\right), \pi_7 = \left(1-\phi+\phi\frac{(\rho\beta_C)_{nf}}{(\rho\beta_C)_w}\right), b = \frac{1-\phi}{S_c}, \tag{12}$$

with stated conditions in the dimensionless form are

$$\begin{aligned} &u(\zeta,0) = 0, T(\zeta,0) = 0, C(\zeta,0) = 0, \zeta \geq 0,\\ &u(0,\tau) = \Lambda(\tau), T(0,\tau) = \Lambda(\tau), (0,\tau) = 1 \text{ where } \Lambda(\tau) = \begin{cases} \tau, & 0 < \tau \leq 1,\\ 1, & \tau > 1, \end{cases}\\ &u(\zeta,\tau) \longrightarrow 0, T(\zeta,\tau) \longrightarrow 0, C(\zeta,\tau) \longrightarrow 0 \text{ as } \zeta \longrightarrow \infty. \end{aligned} \tag{13}$$

3. Solution of the Problem

3.1. Exact Solution of Heat Profile. Applying the definition provided in equation (15) for CF on (6) and plugging equations (8), (9), and (10) yield

$${}^{\mathrm{CF}}D_\tau^\alpha T(\zeta,\tau) = \left(\frac{\pi_5+N_r}{\pi_6 P_r}\right)\frac{\partial^2 T(\zeta,\tau)}{\partial\zeta^2} - \frac{Q}{\pi_6}T(\zeta,\tau), \tag{14}$$

where ${}^{\mathrm{CF}}D_\tau^{\mathfrak{I}}$ is called Caputo–Fabrizio fractional operator [37], and its inverse defined is as follows:

$${}^{\mathrm{CF}}D_t^\wp f(y,t) = \frac{1}{1-\wp}\int_0^t \exp\left(-\frac{\wp(t-\wp)}{1-\wp}\right)\frac{\partial f(y,\tau)}{\partial\tau}\mathrm{d}\tau, \quad 0<\wp<1, \tag{15}$$

$$\mathscr{L}\,{}^{\mathrm{CF}}D_t^\wp f(y,t) = \frac{s\mathscr{L}(f(y,t)) - f(y,0)}{(1-\wp)s+\wp}, \tag{16}$$

where $\wp$ is a fractional parameter. The above equation becomes after employing the Laplace transformation

$$\frac{\partial^2\overline{T}(\zeta,p)}{\partial\zeta^2} - \left(\beta\left(\frac{p}{(1-\alpha)p+\alpha}\right)+\lambda\right)\overline{T}(\zeta,p) = 0, \tag{17}$$

where

$$\beta = \frac{\pi_6 P_r}{\pi_5+N_r}, \lambda = \frac{\mathrm{QP}_r}{\pi_5+N_r}. \tag{18}$$

By using suitable conditions, the (17) has the solution in the form of

$$\begin{aligned} \overline{T}(\zeta,p) &= \left(\frac{1-e^{-p}}{p^2}\right)e^{-\zeta\sqrt{(\beta p/(1-\alpha)p+\alpha+\lambda)}},\\ &= \left(\frac{1-e^{-p}}{p^2}\right)e^{-\zeta\sqrt{\left(b_2 p/p+\eta_2+\lambda\right)}},\\ &= \left(\frac{e^{-\zeta\sqrt{\left(b_2 p/p+\eta_2+\lambda\right)}}}{p^2}\right) - e^{-p}\left(\frac{e^{-\zeta\sqrt{\left(b_2 p/p+\eta_2+\lambda\right)}}}{p^2}\right) = \overline{T_r}(\zeta,p) - e^{-p}\overline{T_r}(\zeta,p). \end{aligned} \tag{19}$$

After applying inverse Laplace transformation on the above equation, we get the solution

$$T(\zeta,\tau) = T_r(\zeta,\tau) - T_r(\zeta,\tau_0)G(\tau_0), \tag{20}$$

where

$$\begin{aligned} T_r(\zeta,\tau) &= L^{-1}\left(\frac{e^{-\zeta\sqrt{(\lambda+\psi p/1+\epsilon p)}}}{p^2}\right), \\ &= \frac{\psi}{\epsilon}\int_0^{\infty}\int_0^{\tau} e^{-\frac{(w\psi+z)}{\epsilon}} erfc\left(\frac{\zeta}{2\sqrt{z}}\right) I_0\left(\frac{2}{\epsilon}\sqrt{(\psi-\lambda\epsilon)wz}\right)\mathrm{d}z\mathrm{d}w \\ &+ \frac{\lambda}{\epsilon}\int_0^{\infty}\int_0^{\nu}\int_0^{\tau} e^{-\frac{(w(1+\lambda)+p)}{\epsilon}} erfc\left(\frac{\zeta}{2\sqrt{z}}\right) I_0\left(\frac{2}{\epsilon}\sqrt{(\psi-\lambda\epsilon)qw}\right)\mathrm{d}z\mathrm{d}q\mathrm{d}w, \end{aligned} \tag{21}$$

$G(\tau_0)$ represent a standard Heaviside function with

$$\tau_0 = \tau - 1, b_2 = \frac{\beta}{1-\alpha}, \eta_2 = \frac{\alpha}{1-\alpha}, \psi = \frac{b_2+\lambda}{\eta_2}, \epsilon = \frac{1}{\eta_2}. \tag{22}$$

It is noticed that when $\alpha \longrightarrow 1$, the results derived by CF in (14) for ramped wall temperature distribution are the same as those obtained by Talha Anwar et al. [55], which proves the validity of the derived results with the published literature.

3.2. Exact Solution of Mass Profile. Applying the definition provided in equation (15) for CF on equation (3) and plugging equations (3), (9), and (10) yield

$${}^{\mathrm{CF}}D_\tau^\alpha C(\zeta,\tau) = \left(\frac{1-\phi}{S_c}\right)\frac{\partial^2 C(\zeta,\tau)}{\partial\zeta^2}. \tag{23}$$

The above equation becomes after employing the Laplace transformation

$$\frac{\partial^2\overline{C}(\zeta,p)}{\partial\zeta^2} - b\left(\frac{p}{(1-\alpha)p+\alpha}\right)\overline{C}(\zeta,p) = 0. \tag{24}$$

By using the equation, the (11) has the solution in the form

$$\overline{C}(\zeta,p) = \left(\frac{1}{p}\right)e^{-\zeta\sqrt{(bp/(1-\alpha)p+\alpha)}}. \tag{25}$$

Employing inverse Laplace transformation, the exact solution for concentration is written as

$$\begin{aligned} C(\zeta,\tau) &= L^{-1}\left(\frac{e^{-\zeta\sqrt{(bp/(1-\alpha)p+\alpha)}}}{p}\right), \\ &= 1 - \frac{2b}{\pi}\int_0^{\infty}\frac{\sin(\zeta/\sqrt{1-\alpha}\chi)}{\chi\left(b+\chi^2\right)}e^{\left(-\alpha/1-\alpha t\chi^2\right)}\mathrm{d}\chi. \end{aligned} \tag{26}$$

3.3. Exact Solution of Velocity Profile. Applying CF fractional time derivative operator as mentioned in equation (15) on (5) gives

$$\begin{aligned} \eta\,{}^{\mathrm{CF}}D_\tau^\alpha u(\zeta,\tau) &= \frac{\partial^2 u(\zeta,\tau)}{\partial\zeta^2} + mG_rT(\zeta,\tau) \\ &+ nG_mC(\zeta,\tau) - wu(\zeta,\tau). \end{aligned} \tag{27}$$

We employ Laplace transformation on the above equation and equations (8), (9), and (10) which gives

$$\begin{aligned} \frac{d^2\overline{u}(\zeta,p)}{d\zeta^2} - \left(\frac{\eta p}{(1-\alpha)p+\alpha} + w\right)\overline{u}(\zeta,p) \\ = -mG_r\overline{T}(\zeta,\tau) - nG_m\overline{C}(\zeta,\tau), \end{aligned} \tag{28}$$

where

$$\eta = \frac{\pi_1}{\pi_4}, w = M\frac{\pi_3}{\pi_4} + \frac{1}{K}, m = \frac{\pi_2}{\pi_4}, n = \frac{\pi_7}{\pi_4}. \tag{29}$$

The result of the homogeneous part of velocity (28) is

$$\overline{u_c}(\zeta,p) = c_1e^{\zeta\sqrt{\eta_1 p/p+\eta_2+w}} + c_2e^{-\zeta\sqrt{\eta_1 p/p+\eta_2+w}}, \tag{30}$$

and the particular solution is written as

$$\begin{aligned} \overline{u_p}(\zeta,p) &= -\frac{mG_r\left(1-e^{-p}/p^2\right)e^{-\zeta\sqrt{b_2p/p+\eta_2+\lambda}}}{\left(b_2p/p+\eta_2+\lambda\right)-\left(\eta_1p/p+\eta_2+w\right)} \\ &- \frac{nG_m(1/p)e^{-\zeta\sqrt{b_1p/p+\eta_2}}}{\left(b_1p/p+\eta_2\right)-\left(\eta_1p/p+\eta_2+w\right)}. \end{aligned} \tag{31}$$

So, the required solution of (28) has the following form:

$$\overline{u}(\zeta,p)=c_1e^{\zeta\sqrt{\eta_1p/p+\eta_2+w}}+c_2e^{-\zeta\sqrt{\eta_1p/p+\eta_2+w}}-\frac{mG_r\left(1-e^{-p}/p^2\right)e^{-\zeta\sqrt{b_2p/p+\eta_2+\lambda}}}{(b_2p/p+\eta_2+\lambda)-(\eta_1p/p+\eta_2+w)}-\frac{nG_m(1/p)e^{-\zeta\sqrt{b_1p/p+\eta_2}}}{(b_1p/p+\eta_2)-(\eta_1p/p+\eta_2+w)}. \tag{32}$$

To find constants c_1 and c_2 by using corresponding conditions, the solution is written as

$$\begin{aligned}\overline{u}(\zeta,p)=&\left(\frac{1-e^{-p}}{p^2}\right)e^{-\zeta\sqrt{\eta_1p/p+\eta_2+w}}+\frac{mG_r(1-e^{-p})(p+\eta_2)}{p^2(b_3p+b_4)}\left[e^{-\zeta\sqrt{\eta_1p/p+\eta_2+w}}-e^{-\zeta\sqrt{b_2p/p+\eta_2+\lambda}}\right]\\&+\frac{nG_m(p+\eta_2)}{p(b_5p-b_6)}\left[e^{-\zeta\sqrt{\eta_1p/p+\eta_2+w}}-e^{-\zeta\sqrt{b_1p/p+\eta_2}}\right],\end{aligned} \tag{33}$$

where

$$\begin{aligned}&\eta_1=\frac{\eta}{1-\alpha},\eta_2=\frac{\alpha}{1-\alpha},b_1=\frac{b}{1-\alpha},b_2=\frac{\beta}{1-\alpha},\\&b_3=b_2-\eta_1+\lambda-w,b_4=(\lambda-w)\eta_2,b_5\\&\quad=b_1-\eta_1-w,b_6=w\eta_2.\end{aligned} \tag{34}$$

Equation (33) can be written in a more precise form as

$$\begin{aligned}\overline{u}(\zeta,p)=&\Phi(\zeta,p)-e^{-p}\Phi(\zeta,p)+\frac{mG_r}{b_3}\left[\Phi(\zeta,p)-e^{-p}\Phi(\zeta,p)-\overline{T}(\zeta,p)\right]\\&+\frac{mG_r\eta_4}{b_3}\left[\delta(\zeta,p)\Phi(\zeta,p)-e^{-p}\delta(\zeta,p)\Phi(\zeta,p)-\delta(\zeta,p)\overline{T}(\zeta,p)\right]\\&+\frac{nG_m}{b_5}\left[\mu(\zeta,p)-\overline{C}(\zeta,p)\right]+\frac{nG_m\eta_6}{b_5}\left[\varphi(\zeta,p)\mu(\zeta,p)-\varphi(\zeta,p)\overline{C}(\zeta,p)\right].\end{aligned} \tag{35}$$

After applying inverse Laplace transformation on the above equation, we get the solution

$$\begin{aligned}u(\zeta,\tau)=&\Phi(\zeta,\tau)-\Phi(\zeta,\tau_0)G(\tau_0)+\frac{mG_r}{b_3}\left[\Phi(\zeta,\tau)-\Phi(\zeta,\tau_0)G(\tau_0)-T(\zeta,\tau)\right]\\&+\frac{mG_r\eta_4}{b_3}\left[\Upsilon(\zeta,\tau)-\Upsilon(\zeta,\tau_0)G(\tau_0)-(\delta*T)(\tau)\right]\\&+\frac{nG_m}{b_5}\left[\mu(\zeta,\tau)-C(\zeta,\tau)\right]+\frac{nG_m\eta_6}{b_5}\left[(\varphi*\mu)(\tau)-(\varphi*C)(\tau)\right],\end{aligned} \tag{36}$$

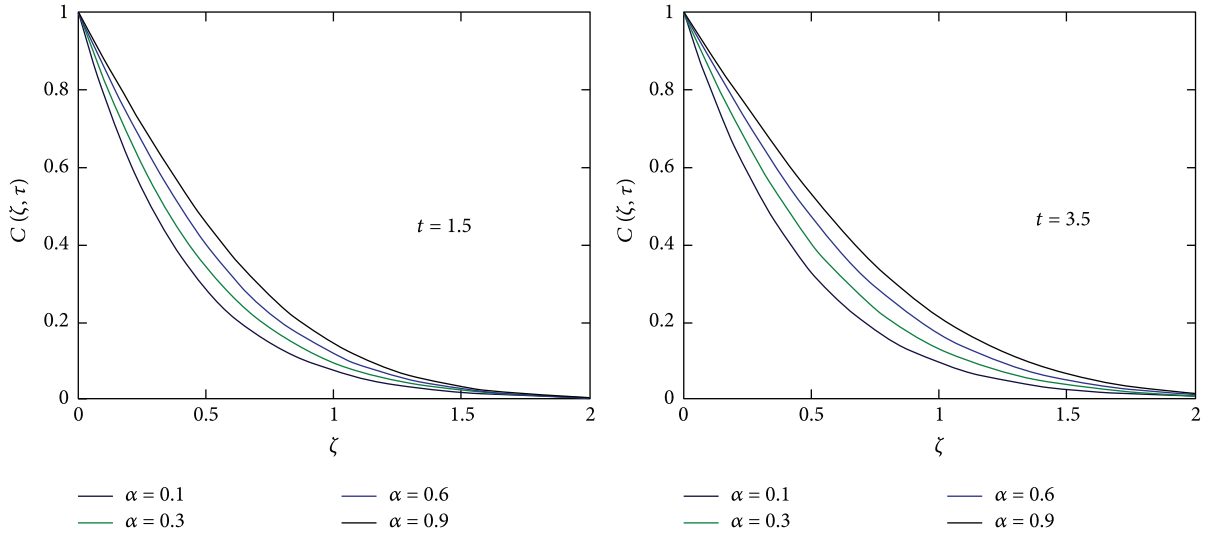

Figure 2: Concentration behavior for different values of α when $\phi = 0.1$, Sc = 3.

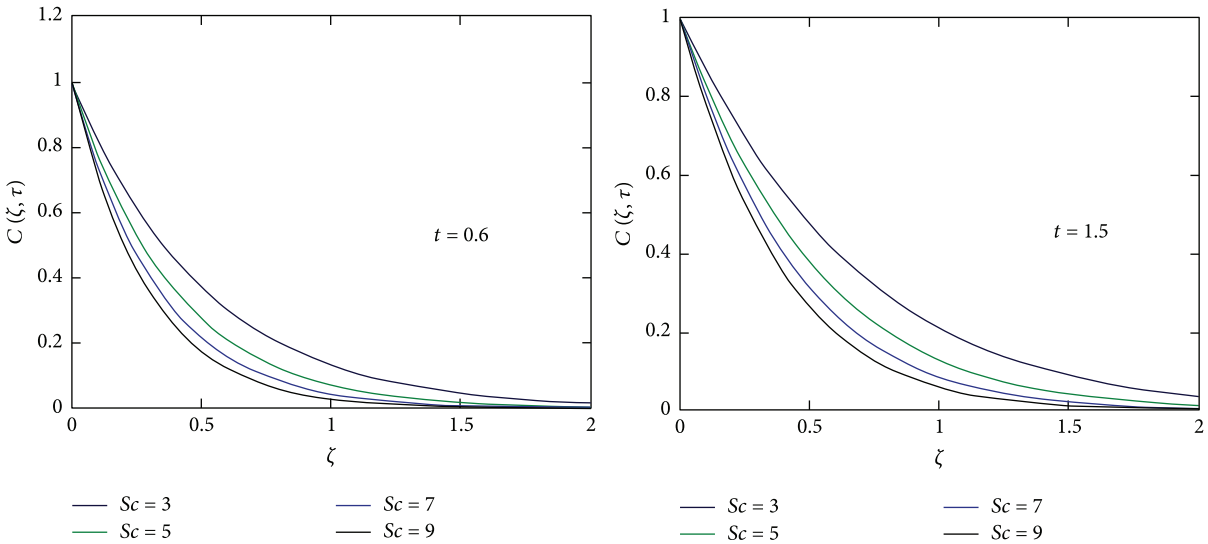

Figure 3: Concentration behavior of Sc for two distinct values of t when $\phi = 0.1, \alpha = 0.3$.

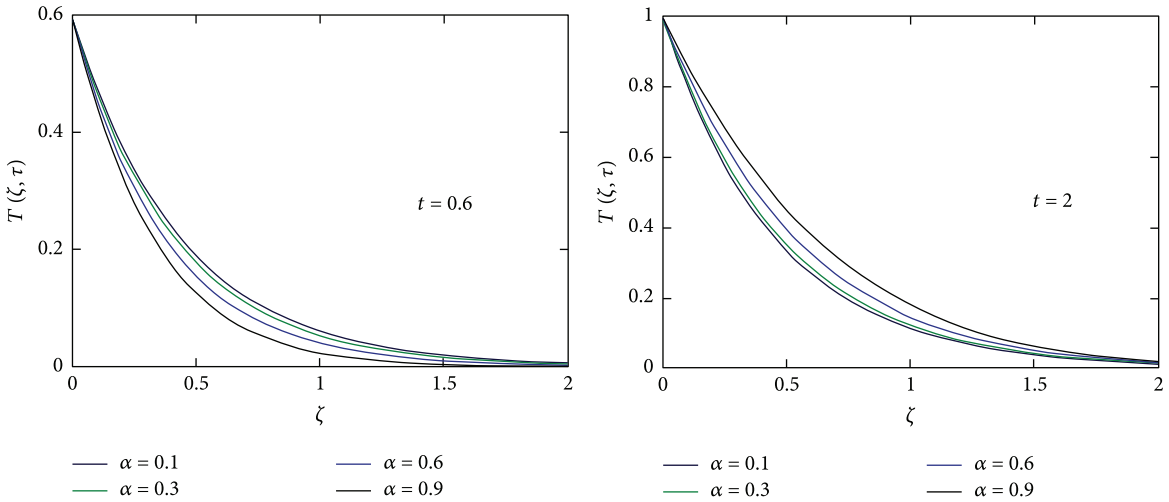

Figure 4: Temperature behavior for different values of α when Pr = 6.2, $\phi = 0.1$, $Q = 0.4$, Nr = 0.5.

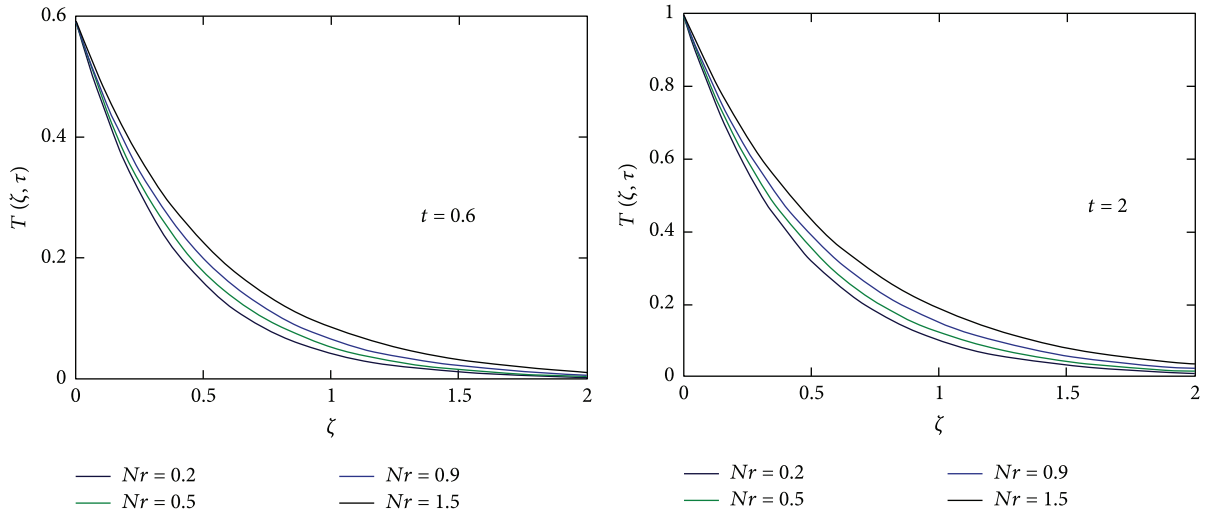

Figure 5: Temperature behavior for two distinct time levels of t for Nr when Pr = 6.2, $\alpha = 0.3$, $Q = 0.4$.

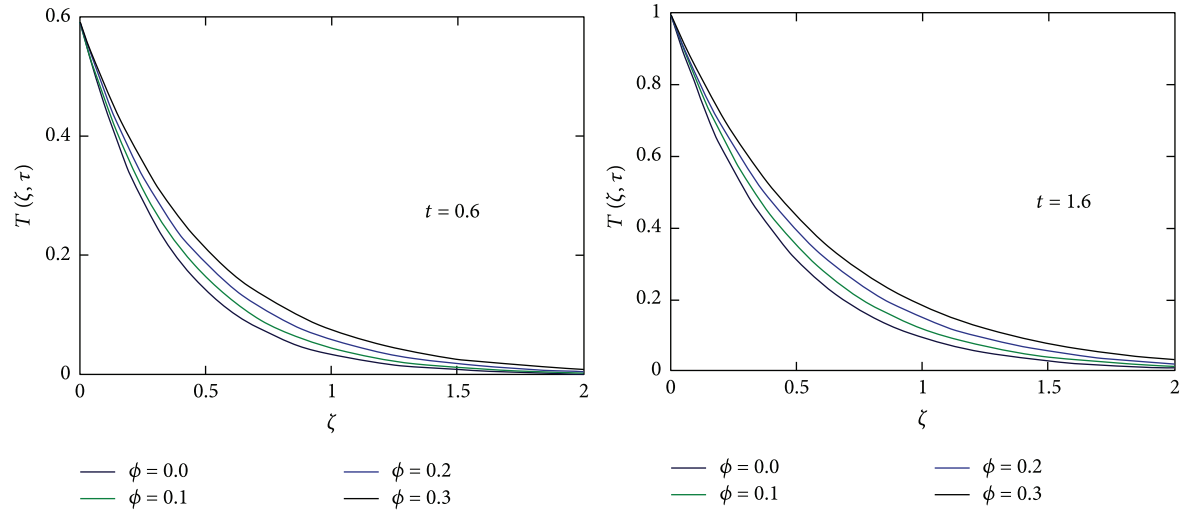

Figure 6: Temperature behavior for two different values of ϕ when Pr = 6.2, $\alpha = 0.3$,$Q = 0.5$, Nr = 0.5.

where

$$\begin{aligned}\Phi(\zeta,\tau) &= L^{-1}\left(\frac{e^{-\zeta\sqrt{(w+\gamma p/1+\epsilon p)}}}{p^2}\right),\\ &= \frac{\gamma}{\epsilon}\int_0^{\infty}\int_0^{\tau} e^{-\frac{(s\gamma+z)}{\epsilon}}\, erfc\left(\frac{\zeta}{2\sqrt{z}}\right) I_0\left(\frac{2}{\epsilon}\sqrt{(\gamma-w\epsilon)sz}\right)\mathrm{d}z\mathrm{d}s\\ &+ \frac{w}{\epsilon}\int_0^{\infty}\int_0^{\gamma}\int_0^{\tau} e^{-\frac{(s(1+w)+p)}{\epsilon}}\, erfc\left(\frac{\zeta}{2\sqrt{z}}\right) I_0\left(\frac{2}{\epsilon}\sqrt{(\gamma-w\epsilon)qs}\right)\mathrm{d}z\mathrm{d}q\mathrm{d}s,\end{aligned} \tag{37}$$

and $G(\tau_0)$ represent a standard Heaviside function with

$$\tau_0 = \tau - 1, b_2 = \frac{\beta}{1-\alpha}, \eta_2 = \frac{\alpha}{1-\alpha}, \psi = \frac{b_2 + \lambda}{\eta_2}, \gamma = \frac{\eta_1 + w}{\eta_2}$$

$$\epsilon = \frac{1}{\eta_2}, \eta_3 = -\frac{b_4}{b_3}, \eta_4 = \eta_2 + \eta_3, \eta_5 = \frac{b_6}{b_5}, \eta_6 = \eta_2 + \eta_5,$$

$$\delta(\zeta,\tau) = L^{-1}\left[\frac{1}{p-\eta_3}\right] = e^{\eta_3\tau}, \varphi(\zeta,\tau) = L^{-1}\left[\frac{1}{p-\eta_5}\right] = e^{\eta_5\tau}, \Upsilon(\zeta,\tau) = (\delta * \Phi)(\tau), \tag{38}$$

$$\mu(\zeta,\tau) = L^{-1}\left(\frac{e^{-\zeta\sqrt{(w+\gamma p/1+\epsilon p)}}}{p}\right),$$

$$= e^{-\zeta\sqrt{w}} - \frac{\zeta\sqrt{\gamma}}{2\pi}\int_0^\infty \int_0^\tau \frac{1}{\sqrt{\tau}} e^{-\left(\epsilon\tau + \zeta^2/4\nu + w\nu\right)} I_1\left(2\sqrt{\gamma\nu\tau}\right) d\tau d\nu.$$

It is detected that when $\alpha \longrightarrow 1$ and $Gm = 0$, the fractionalized model CF in equation (3) for ramped wall velocity profile is converted into integer order model as calculated by Talha Anwar et al. [55]. Also, we achieved the same results as Seth et al. [29] for ramped wall temperature with $\phi = 0$ and $Gm = 0$. Moreover, we derived similar solutions as obtained by Chandran et al. [28] when porosity parameter $1/K \longrightarrow 0$, $Gm = 0$, and magnetic parameter $M \longrightarrow 0$. This authenticates the current acquired results with the published literature.

4. Results and Discussion

In order to achieve the goal of having a comprehensive understanding of the physical mechanism of current problem completely, a parametric analysis is performed, and computed solutions are revealed with the assistance of graphs. In this section, the influence of many pertinent parameters such as $\phi, Gr, M, K, Gm, Nr, Sc$, and fractional parameter α an obtained solution of water base nanoparticles with ramped conditions subject to the application of different fractional operators CF is studied by using MARHCAD-15 software.

It is observed that temperature, concentration, and velocity profile are controlled by the fractional parameter α. Figures 2 and 3 illustrate for different time levels the effect of fractional parameter α and Sc on concentration. For small and large values of time t and using different values of fractional parameter α, it is observed from Figure 2 that the behavior of concentration is increasing for a small time and decreasing for a large time. Also, Figure 3 illustrates the behavior of concentration for Sc at two different values of time, and it is observed that concentration is decreasing as the value of Sc is increasing. Figure 4 displays the temperature decreasing for a small time and increasing for a large time, using various values of the fractional parameter α. It is detected that increasing the values of radiation parameter Nr elevates the temperature distribution for a small and large time in Figure 5. The impact of nanoparticle solid volume fraction ϕ is analyzed on temperature distribution for varying times in Figure 6. A raise in the solid volume fraction parameter elevates the temperature contour. Indeed, an increase in the value of ϕ increased fluid density and cause to increase in the thickness of the boundary layer which helps to improve the thermal conductivity and surface heat transfer rate is also increased.

Figure 7 displays the graphs of nanofluid velocity for different values of Gr with various values of fractional parameter α. It is noticed that the velocity profile is elevated corresponding to rising values of Gr. It is observed that the velocity and Gr have direct relation. Generally, Gr deals with buoyancy and viscous forces, and the strength of the viscous force is decreased due to a raise in Gr. Consequently, nanofluid velocity is elevated when it is close to an oscillating plate, and then, the nanofluid flow is apart from the plate, forces become delicate, and gradually, the motion of fluid approaches zero. In Figure 8, four different graphs are drawn for dissimilar values of Gm and numerous values of the fractional parameter α. The mass Grashof number is the ratio of mass buoyancy force to viscous force, which causes free convection. It is noted that the fluid velocity is increasing if we increase the value of G_m.

In Figure 9, the graphs of nanofluid velocity for different values of Sc are displayed, with various values of fractional parameter α. It is observed that the velocity profile is decreased corresponding to increasing values of Sc. In Figure 10, it is analyzed that velocity is elevated for different values of K using various values of fractional parameter α. So, Figure 10 shows the relationship between dimensionless velocity and permeability parameter K which highlights the fact that nanofluid velocity is accelerated correspondingly to increase the values of K for CF fractional operator varying fractional parameter α.

In Figure 11, it is analyzed that four different graphs are traced for fixed time, but different values of M and various values of fractional parameter α via CF the velocity is

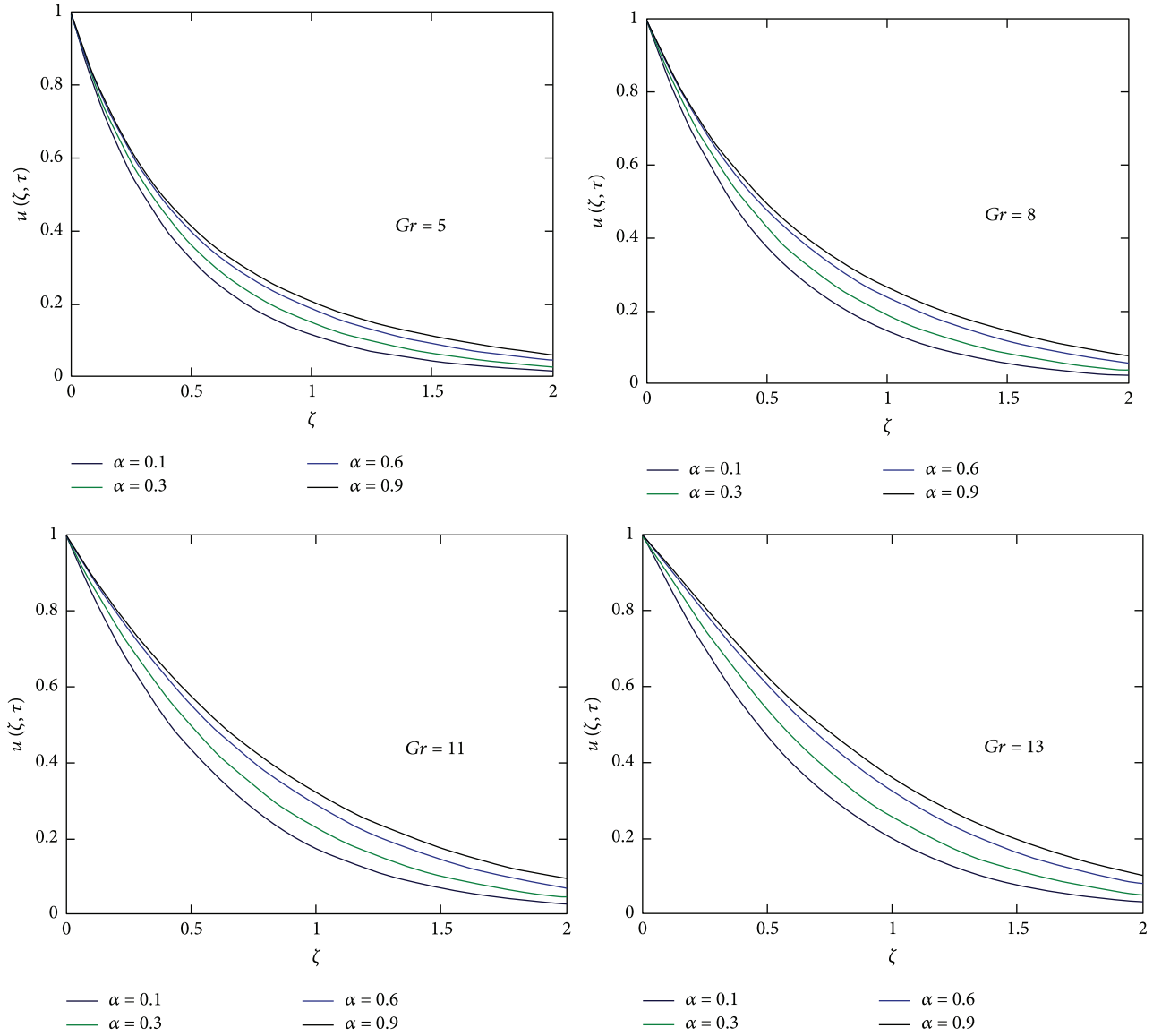

Figure 7: Velocity behavior for four different values of Gr via ABC when Pr = 6.2, $\phi = 0.1$, Gm = 0.25, Sc = 3, $M = 2$, $Q = 0.5$, Nr = 0.5, $K = 0.5$.

decreased. In Figure 12, the impact of fractional parameter is investigated on nanofluid velocity at two different levels of time. For small and large values of time t and using different values of fractional parameter α, it is observed that the behavior of velocity is decreasing for a small time and increasing for greater values of the time. This rapid decay in velocity is due to an increase in momentum boundary layer for increasing α. It is inspected that temperature and velocity profile is controlled by a time-fractional parameter. It is observed that the variation of fractional parameter α on the nanofluids velocity profile and comparison between the CF factional model with an ordinary model is discussed in Figure 13. The velocity profile is reduced by increasing the value of the fractional parameter α. In Figure 14, it is noticed that when $\alpha \longrightarrow 1$, the CF fractional model becomes an ordinary model.

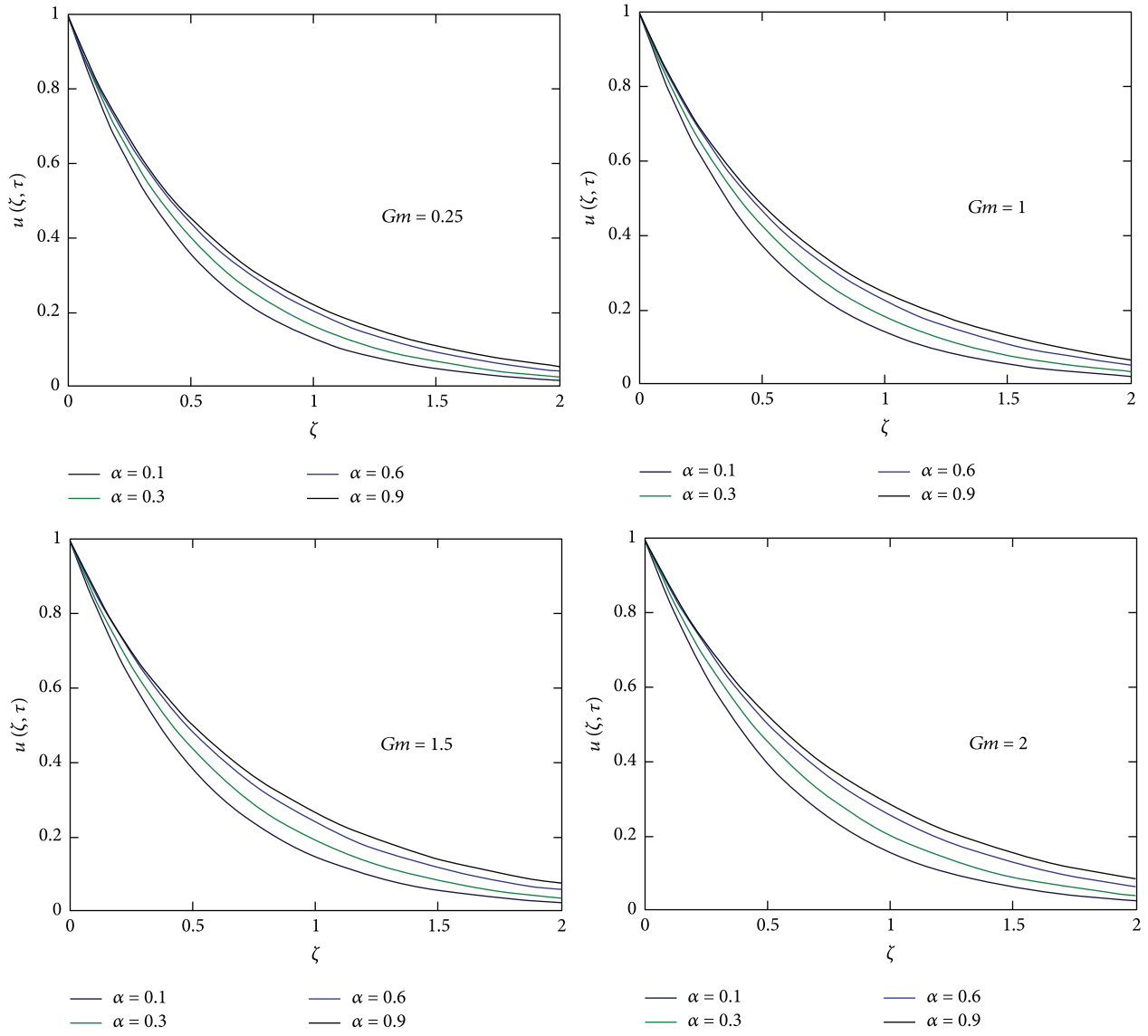

Figure 8: Velocity behavior for four distinct values of Gm when $\phi = 0.3$, $t = 5$, $M = 2$, $Q = 0.5$, Gr = 5, Sc = 3, $K = 2$, Pr = 6.2, Nr = 0.5, $K = 0.5$.

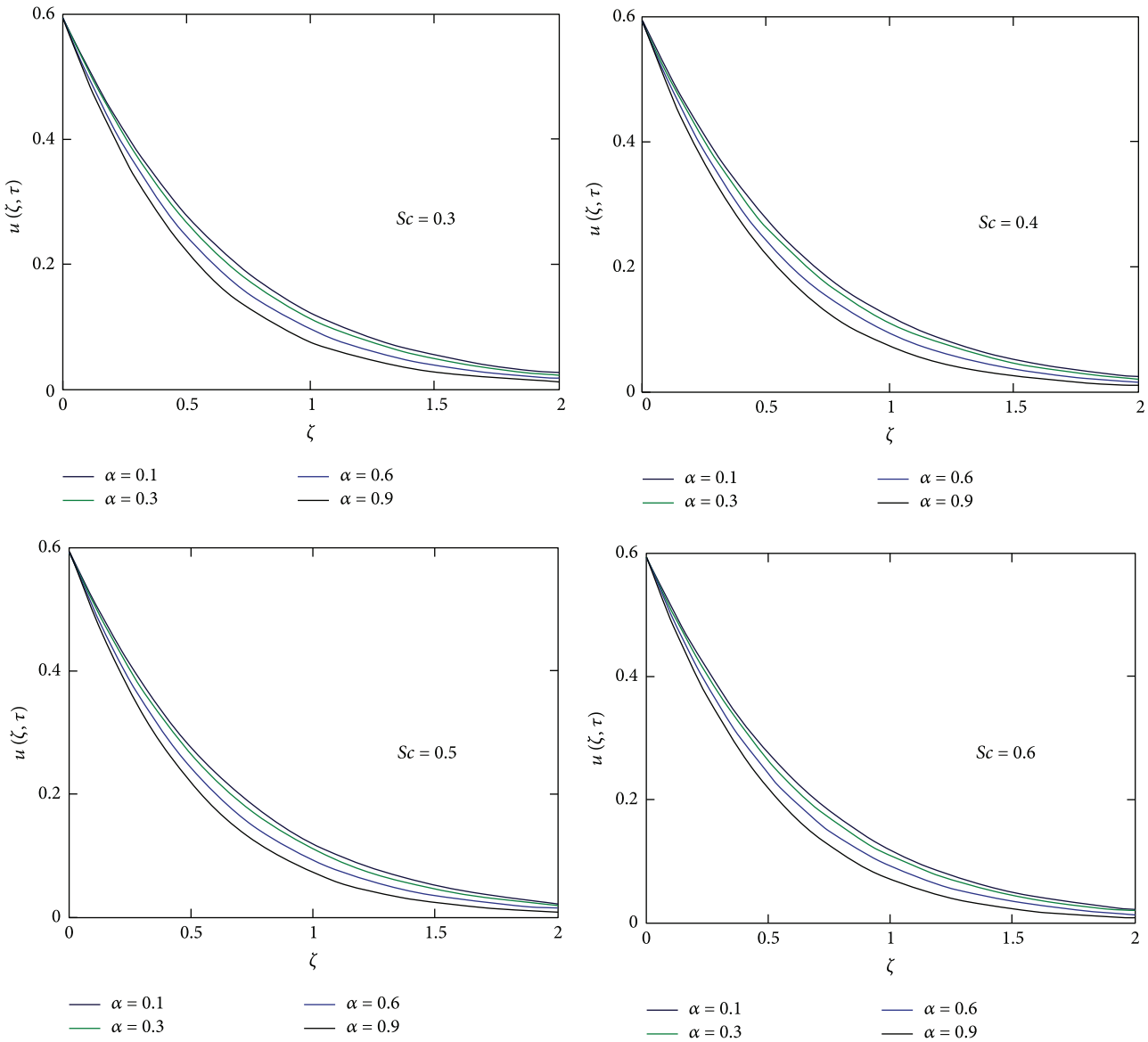

Figure 9: Velocity behavior for four different values of Sc when $\phi = 0.3$, $t = 5$, $M = 2$, Gm = 0.25, Gr = 5, $Q = 0.5$, Nr = 0.5, Pr = 6.2, $K = 0.5$.

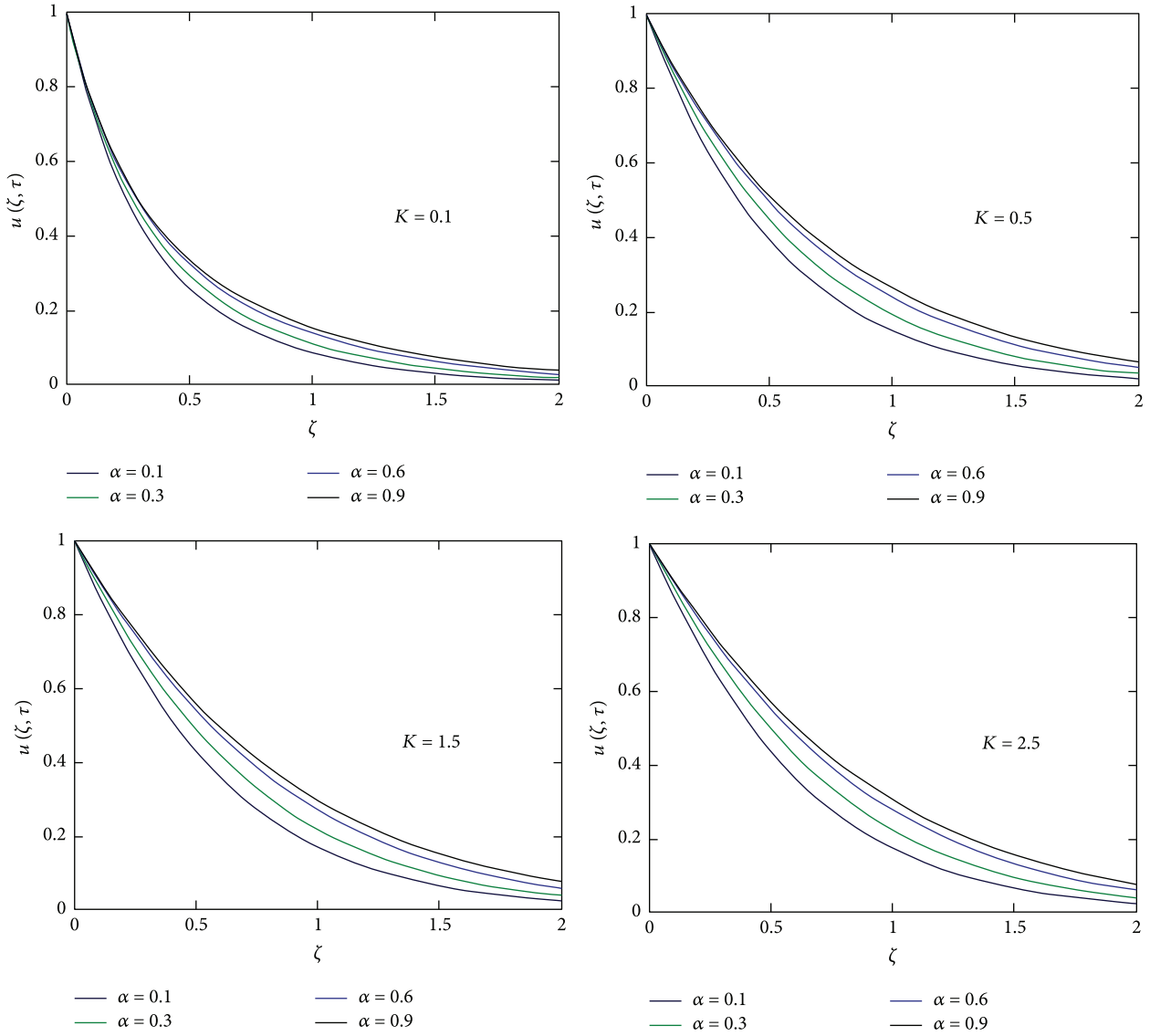

Figure 10: Velocity behavior for two different values of K when Pr = 6.2, $\phi = 0.1$, $t = 5$, $M = 7$, Gm = 0.25, Sc = 3, $Q = 0.4$, Nr = 0.5, Gr = 15.

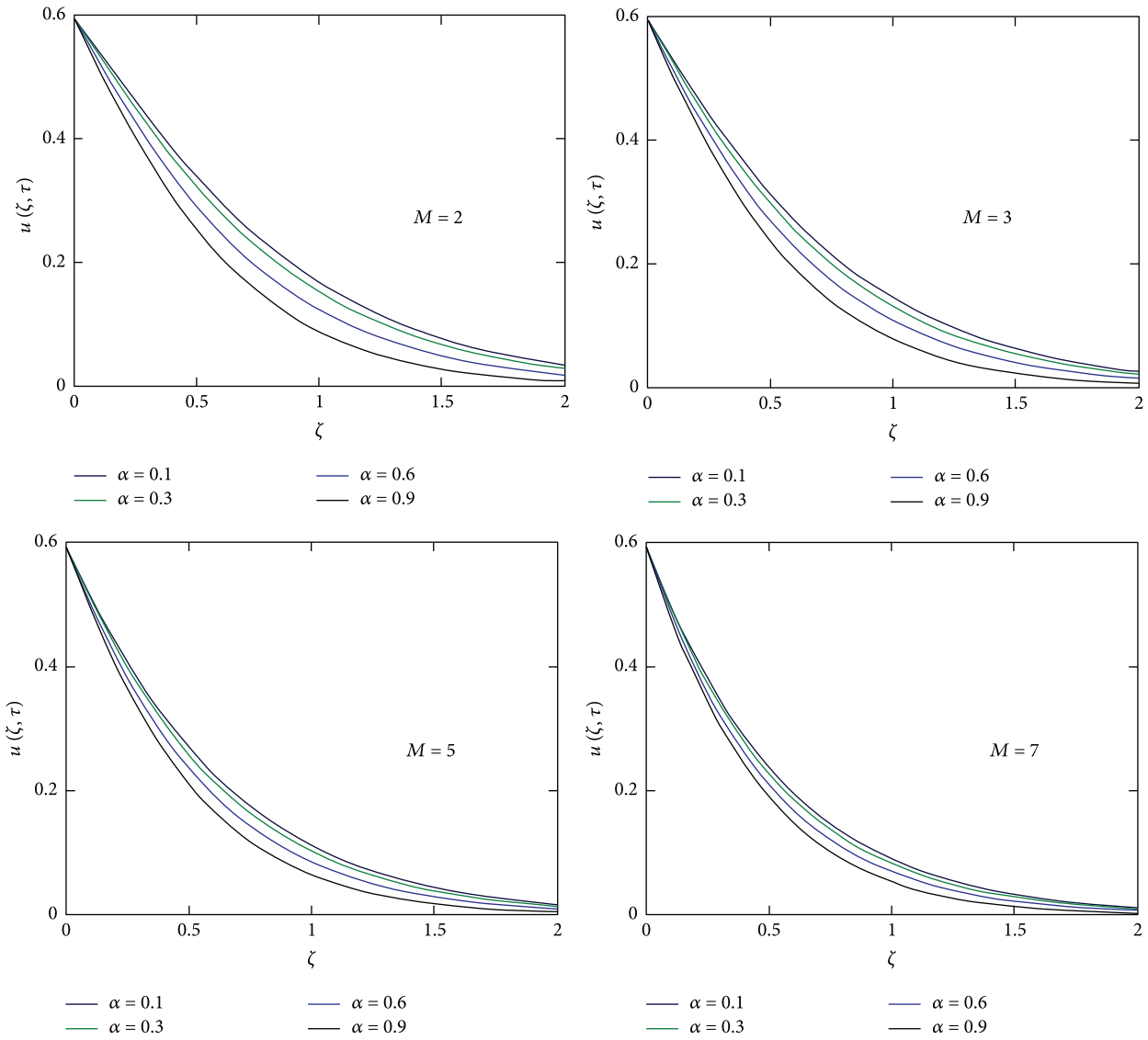

FIGURE 11: Velocity comparison between CF and ordinary model when Pr = 6.2, $\phi = 0.1$, $t = 0.35$, Gm = 0.25, Sc = 3, $K = 2$, $Q = 0.5$, Nr = 0.5, Gr = 5.

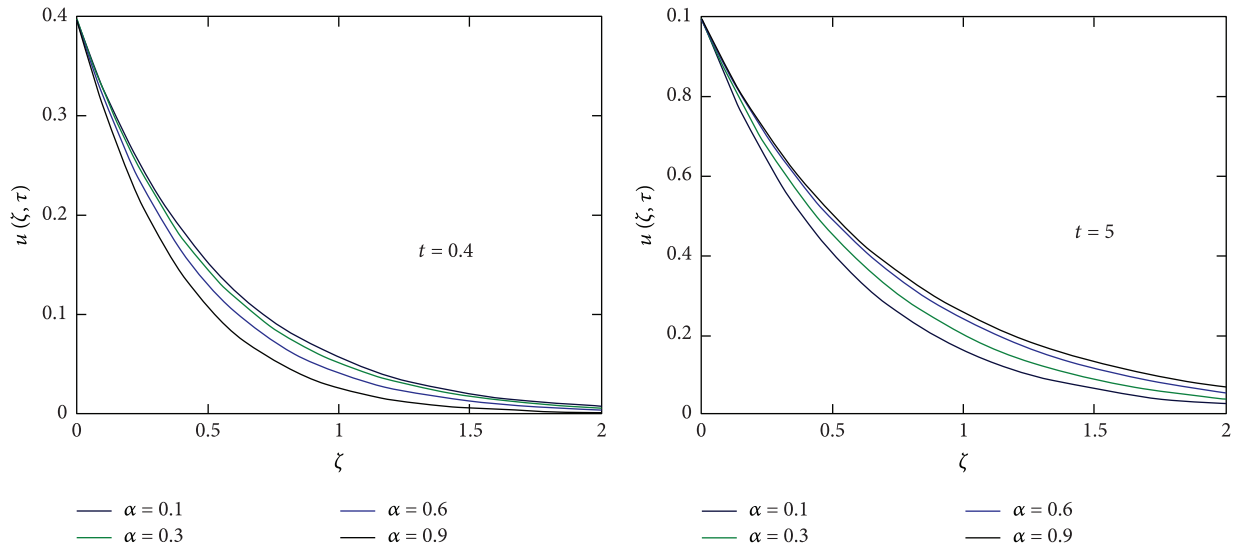

Figure 12: Velocity behavior for different values of α when Pr = 6.2, $\phi = 0.1$, $t = 0.35$,$M = 2$, Gm = 0.25, Sc = 3, $Q = 0.5$, Nr = 0.5, $K = 3$, Gr = 5.

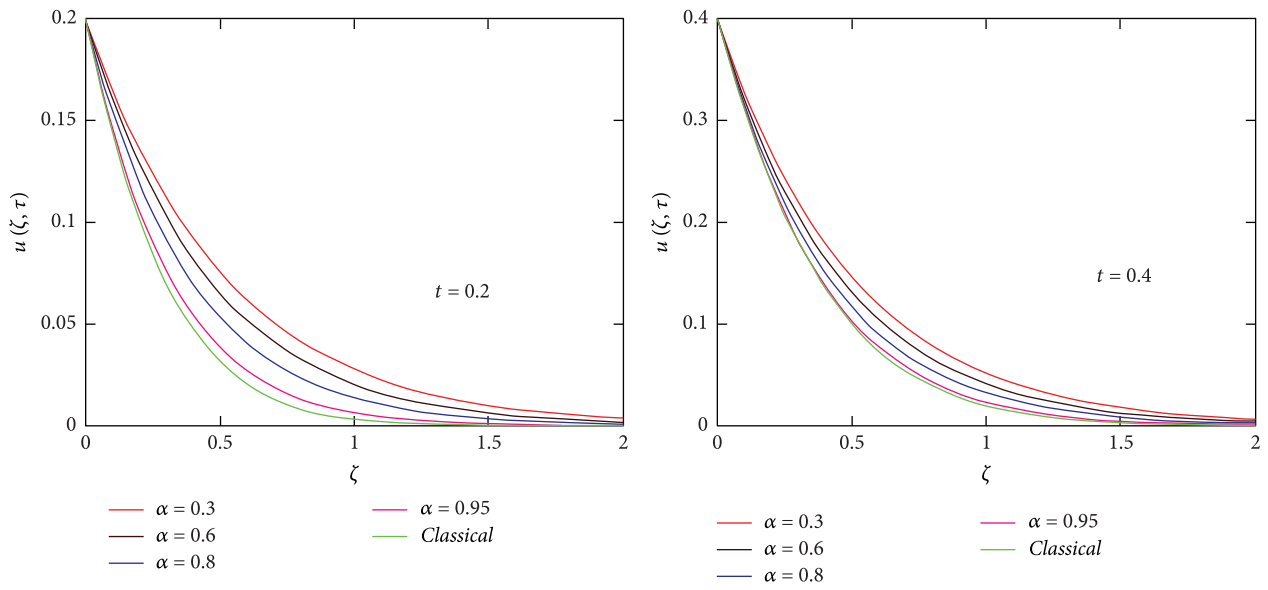

Figure 13: Velocity comparison between CF and ordinary model when Pr = 6.2, $\phi = 0.1$, $t = 0.35$, $M = 2$, Gm = 0.25, Sc = 3, $Q = 0.5$, Nr = 0.5, Gr = 5.

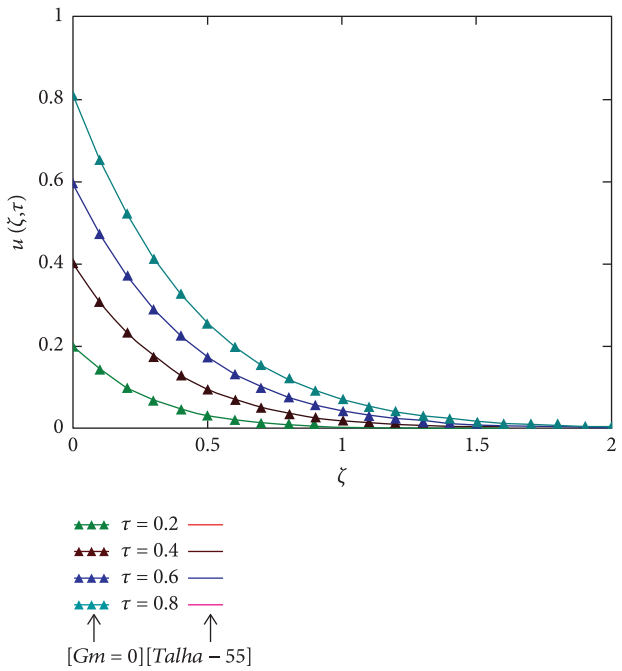

Figure 14: Velocity comparison with [55].

5. Conclusion

The comprehensive analysis of the time fractional derivative with heat and mass transfer to evaluate the physical effects of application of simultaneous ramped wall velocity and ramped wall temperature condition on unsteady, MHD convection flow of some nanofluids. In addition, heat injection/consumption and heat radiative flux are also inculcated in the model. However, in this work, exact and closed-form solutions are derived by employing the Laplace transformation. For physical significance, the graphs of various system parameters are demonstrated. The following major findings of this study are given as follows:

(i) The temperature profile increases due to enlargement in volume fraction ϕ and by increasing the value of N_r also noted that decay in concentration profile by enhancing the values of S_c.

(ii) Nanofluid velocity is a decreasing function of magnetic parameter M.

(iii) It is observed that the effect of α for small and large time on temperature, concentration, and velocity profile is quite opposite.

(iv) For the greater value of K, velocity profile is elevated for varying fractional parameter α for fractional operator applied on nanofluid velocity also noted that decay in velocity for growing values of the S_c.

(v) Velocity profile enhances by increasing the values of Gr and Gm for a fixed time and different values of α.

(vi) CF time-fractional operator converges to ordinary model when $\alpha \longrightarrow 1$.

(vii) In the future, we solved this fractionalized problem through a numerical approach with different techniques. Also, we solved this viscous model via other conditions.

Nomenclature

V: Fluid velocity vector
J: Current density
B: Total magnetic field
r: Darcy resistant vector
ρ: Fluid density
t: Time
g: Force of gravity
β: Thermal expansion coefficient
K_f: Thermal conductivity of fluid
γ_1: Viscous dissipation term
Gr: Grashot number
M: Magnetic parameter
Nr: Radiation parameter
Pr: Prandtl number
K: Permeability parameter
C_p: Specific heat capacitance
Q_r: Thermal radiation flux
Q: Heat injection/consumption constant
k^*: Porosity term
E: Electric field
B_0: Imposed magnetic field
t_0: Characteristic time
ϕ: Nanoparticle volume fraction
k_r: Coefficient of rosseland adsorption
u: Dimensionless velocity
Q_0: Heat injection/consumption parameter
$\mathscr{L}$: Laplace transform operator
$\mathscr{L}^{-1}$: Laplace transform operator.

Data Availability

No data were used to support this study.

Conflicts of Interest

The author professed that there are no conflicts of interest for this publication, research, and authorship of this article.

Acknowledgments

The authors are highly obliged and appreciative for support of this research article to the Lahore, Pakistan.

References

[1] S. U. S. Choi, "Enhancing thermal conductivity of fluids with nanoparticles. International mechanical engineering congress and exposition, San Francisco, USA," *ASME, FED*, vol. 66, pp. 99–105, 1995.

[2] V. Di Sarli, G. Landi, L. Lisi, and A. Di Benedetto, "Ceria-coated diesel particulate filters for continuous regeneration," *AIChE Journal*, vol. 63, no. 8, pp. 3442–3449, 2017.

[3] H. Masuda, A. Ebata, K. Teramae, N. Hishinuma, and Y. Ebata, "Alteration of thermal conductivity and viscosity of

liquid by dispersing ultra-fine particles. Dispersion of Al2O3, SiO2 and TiO2 ultra-fine particles," *Netsu Bussei*, vol. 7, no. 4, pp. 227–233, 1993.

[4] S. K. Das, N. Putra, P. Thiesen, and W. Roetzel, "Temperature dependence of thermal conductivity enhancement for nanofluids," *Journal of Heat Transfer*, vol. 125, no. 4, pp. 567–574, 2003.

[5] M. A. A. Hamad, I. Pop, and A. Md Ismail, "Magnetic field effects on free convection flow of a nanofluid past a vertical semi-infinite flat plate," *Nonlinear Analysis: Real World Applications*, vol. 12, no. 3, pp. 1338–1346, 2011.

[6] S. Das and R. N. Jana, "Natural convective magneto-nanofluid flow and radiative heat transfer past a moving vertical plate," *Alexandria Engineering Journal*, vol. 54, no. 1, pp. 55–64, 2015.

[7] M. Turkyilmazoglu, "Exact analytical solutions for heat and mass transfer of MHD slip flow in nanofluids," *Chemical Engineering Science*, vol. 84, pp. 182–187, 2012.

[8] M. Sheikholeslami and D. D. Ganji, "Numerical investigation for two phase modeling of nanofluid in a rotating system with permeable sheet," *Journal of Molecular Liquids*, vol. 194, pp. 13–19, 2014.

[9] A. Hussanan, I. Khan, H. Hashim et al., "Unsteady MHD flow of some nanofluids past an accelerated vertical plate embedded in a porous medium," *Jurnal Teknologi*, vol. 78, no. 2, pp. 121–126, 2016.

[10] M. S. Anwar and A. Rasheed, "Joule heating in magnetic resistive flow with fractional Cattaneo-Maxwell model," *Journal of the Brazilian Society of Mechanical Sciences and Engineering*, vol. 40, no. 10, p. 501, 2018.

[11] A. Rasheed and M. Shoaib Anwar, "Interplay of chemical reacting species in a fractional viscoelastic fluid flow," *Journal of Molecular Liquids*, vol. 273, pp. 576–588, 2019.

[12] M. Irfan, M. S. Anwar, M. Rashid, M. Waqas, and W. A. Khan, "Arrhenius activation energy aspects in mixed convection Carreau nanofluid with nonlinear thermal radiation," *Applied Nanoscience*, vol. 10, no. 12, pp. 4403–4413, 2020.

[13] A. Khan, D. Khan, F. Ali, F. u. Karim, and M. Imran, "MHD flow of sodium alginate-based Casson type nanofluid passing through a porous medium with Newtonian heating," *Scientific Reports*, vol. 8, no. 1, p. 8645, 2018.

[14] A.-C. Ji, W. M. Liu, J. L. Song, and F. Zhou, "Dynamical creation of fractionalized vortices and vortex lattices," *Physical Review Letters*, vol. 101, no. 1, Article ID 010402, 2008.

[15] D.-S. Wang, X.-H. Hu, J. Hu, and W. M. Liu, "Quantized quasi-two-dimensional Bose-Einstein condensates with spatially modulated nonlinearity," *Physical Review A*, vol. 81, no. 2, Article ID 025604, 2010.

[16] R. Cortell, "Fluid flow and radiative nonlinear heat transfer over a stretching sheet," *Journal of King Saud University Science*, vol. 26, no. 2, pp. 161–167, 2014.

[17] C.-F. Liu, Y.-M. Yu, S.-C. Gou, and W.-M. Liu, "Vortex chain in anisotropic spin-orbit-coupled spin-1 Bose-Einstein condensates," *Physical Review A*, vol. 87, no. 6, Article ID 063630, 2013.

[18] B. Jamil, M. S. Anwar, A. Rasheed, and M. Irfan, "MHD Maxwell flow modeled by fractional derivatives with chemical reaction and thermal radiation," *Chinese Journal of Physics*, vol. 67, pp. 512–533, 2020.

[19] N. Ahmed and M. Dutta, "Transient mass transfer flow past an impulsively started infinite vertical plate with ramped plate velocity and ramped temperature," *International Journal of the Physical Sciences*, vol. 8, no. 7, pp. 254–263, 2013.

[20] O. B. e. Silva and D. C. Sobral Filho, "A new proposal to guide velocity and inclination in the ramp protocol for the treadmill ergometer," *Arquivos Brasileiros de Cardiologia*, vol. 81, no. 1, pp. 48–53, 2003.

[21] R. A. Bruce, "Evaluation of functional capacity and exercise tolerance of cardiac patients," *Modern Concepts of Cardiovascular Disease*, vol. 25, pp. 321–326, 1956.

[22] J. Myers and D. Bellin, "Ramp exercise protocols for clinical and cardiopulmonary exercise testing," *Sports Medicine*, vol. 30, no. 1, pp. 23–29, 2000.

[23] C. P. Malhotra, R. L. Mahajan, W. S. Sampath, K. L. Barth, and R. A. Enzenroth, "Control of temperature uniformity during the manufacture of stable thin-film photovoltaic devices," *International Journal of Heat and Mass Transfer*, vol. 49, no. 17-18, pp. 2840–2850, 2006.

[24] J. A. Schetz, "On the approximate solution of viscous-flow problems," *Journal of Applied Mechanics*, vol. 30, no. 2, pp. 263–268, 1963.

[25] A. A. Hayday, D. A. Bowlus, and R. A. McGraw, "Free convection from a vertical flat plate with step discontinuities in surface temperature," *Journal of Heat Transfer*, vol. 89, no. 3, pp. 244–249, 1967.

[26] B. Kundu, "Exact analysis for propagation of heat in a biological tissue subject to different surface conditions for therapeutic applications," *Applied Mathematics and Computation*, vol. 285, pp. 204–216, 2016.

[27] R. Nandkeolyar, M. Das, and H. Pattnayak, "Unsteady hydromagnetic radiative flow of a nanofluid past a flat plate with ramped temperature," *J. Orissa Math. Soc.*vol. 975, p. 2323, 2013.

[28] P. Chandran, N. C. Sacheti, and A. K. Singh, "Natural convection near a vertical plate with ramped wall temperature," *Heat and Mass Transfer*, vol. 41, no. 5, pp. 459–464, 2005.

[29] G. S. Seth, M. S. Ansari, and R. Nandkeolyar, "MHD natural convection flow with radiative heat transfer past an impulsively moving plate with ramped wall temperature," *Heat and Mass Transfer*, vol. 47, no. 5, pp. 551–561, 2011.

[30] K. Hosseinzadeh, S. Salehi, M. R. Mardani, F. Y. Mahmoudi, M. Waqas, and D. D. Ganji, "Investigation of nano-Bioconvective fluid motile microorganism and nanoparticle flow by considering MHD and thermal radiation," *Informatics in Medicine Unlocked*, vol. 21, Article ID 10046, 2020.

[31] D. Baleanu, B. Ghanbari, A. Jajarmi, H. Mohammadi Pirouz, and H. M. Pirouz, "Planar system-masses in an equilateral triangle: numerical study within fractional calculus," *Computer Modeling in Engineering and Sciences*, vol. 124, no. 3, pp. 953–968, 2020.

[32] S. S. Sajjadi, D. Baleanu, A. Jajarmi, and H. M. Pirouz, "A new adaptive synchronization and hyperchaos control of a biological snap oscillator," *Chaos, Solitons & Fractals*, vol. 138, Article ID 109919, 2020.

[33] D. Baleanu, A. Jajarmi, S. S. Sajjadi, and J. H. Asad, "The fractional features of a harmonic oscillator with position-dependent mass," *Communications in Theoretical Physics*, vol. 72, no. 5, Article ID 055002, 2020.

[34] S. Tauseef Saeed, M. Bilal Riaz, D. Baleanu, A. Akg黷, and S. Muhammad, "Exact analysis of second grade fluid with generalized boundary conditions," *Intelligent Automation & Soft Computing*, vol. 28, no. 2, pp. 547–559, 2021.

[35] S. T. Saeed, M. B. Riaz, D. Baleanu, and K. A. Abro, "A mathematical study of natural convection flow through a channel with non-singular kernels: an application to transport phenomena," *Alexandria Engineering Journal*, vol. 59, no. 4, pp. 2269–2281, 2020.

[36] I. Khan, S. T. Saeed, M. B. Riaz, K. A. Abro, S. M. Husnine, and K. S. Nisar, "Influence in a Darcy's medium with heat production and radiation on MHD convection flow via modern fractional approach," *Journal of Materials Research and Technology*, vol. 9, no. 5, pp. 10016–10030, 2020.

[37] A. Atangana and D. Baleanu, "New fractional derivatives with nonlocal and non-singular kernel: t," *Thermal Science*, vol. 20, no. 2, pp. 763–769, 2016.

[38] M. B. Riaz, S. T. Saeed, D. Baleanu, and M. M. Ghalib, "Computational results with non-singular and non-local kernel flow of viscous fluid in vertical permeable medium with variant temperature," *Frontiers in Physics*, vol. 8, p. 275, 2020.

[39] M. B. Riaz, A. Atangana, and S. T. Saeed, "MHD free convection flow over a vertical plate with ramped wall temperature and chemical reaction in view of non-singular kernel," *Fractional Order Analysis*, Wiley, Hoboken, pp. 253–282, 2020.

[40] M. B. Riaz, A. Atangana, and N. Iftikhar, "Heat and mass transfer in Maxwell fluid in view of local and non-local differential operators," *Journal of Thermal Analysis and Calorimetry*, vol. 143, no. 6, pp. 4313–4329, 2020.

[41] M. B. Riaz and N. Iftikhar, "A comparative study of heat transfer analysis of MHD Maxwell fluid in view of local and nonlocal differential operators," *Chaos, Solitons & Fractals*, vol. 132, Article ID 109556, 2020.

[42] A. U. Aziz-Ur-Rehman, M. Bilal Riaz, S. Tauseef Saeed, and S. Yao, "Dynamical analysis of radiation and heat transfer on MHD second grade fluid," *Computer Modeling in Engineering and Sciences*, vol. 129, no. 2, pp. 689–703, 2021.

[43] M. B. Riaz, K. A. Abro, K. M. Abualnaja et al., "Exact solutions involving special functions for unsteady convective flow of magnetohydrodynamic second grade fluid with ramped conditions," *Advances in Difference Equations*, vol. 2021, no. 1, 2021.

[44] A. U. Aziz-Ur-Rehman, M. B. Riaz, J. Awrejcewicz, and D. Baleanu, "Exact solutions for thermomagetized unsteady non-singularized jeffrey fluid: effects of ramped velocity, concentration with Newtonian heating," *Results in Physics*, vol. 26, Article ID 104367, 2021.

[45] A. U. Rehman, M. B. Riaz, A. Akgül, S. T. Saeed, and D. Baleanu, "Heat and mass transport impact on MHD second-grade fluid: a comparative analysis of fractional operators," *Heat Transfer*, vol. 50, no. 7, pp. 7042–7064, 2021.

[46] G. S. Seth, S. M. Hussain, and S. Sarkar, "Hydromagnetic natural convection flow with heat and mass transfer of a chemically reacting and heat absorbing fluid past an accelerated moving vertical plate with ramped temperature and ramped surface concentration through a porous medium," *Journal of the Egyptian Mathematical Society*, vol. 23, no. 1, pp. 197–207, 2015.

[47] N. Iftikhar, S. T. Saeed, and M. B. Riaz, "Fractional study of heat and mass transfer of MHD Oldroyd-B fluid with ramped velocity and temperature," *Comp Methods Diff Equ*, vol. 10, pp. 1–28, 2021.

[48] K. Hosseinzadeh, M. R. Mardani, S. Salehi, M. M. Paikar, and D. D. Ganji, "Entropy generation of three-dimensional Bödewadt flow of water and hexanol base fluid suspended by $$\hbox {Fe}_{{{3}}}\hbox {O}_{{{4}}}$$ and $$\hbox {MoS}_{{{2}}}$$ hybrid nanoparticles," *Pramana*, vol. 95, no. 2, p. 57, 2021.

[49] K. Hosseinzadeh, S. Roghani, A. R. Mogharrebi, A. Asadi, M. Waqas, and D. D. Ganji, "Investigation of cross-fluid flow containing motile gyrotactic microorganisms and nanoparticles over a three-dimensional cylinder," *Alexandria Engineering Journal*, vol. 59, no. 5, pp. 3297–3307, 2020.

[50] K. Hosseinzadeh, S. Roghani, A. R. Mogharrebi, and A. D. D. Asadi, "Optimization of hybrid nanoparticles with mixture fluid flow in an octagonal porous medium by effect of radiation and magnetic field," *Journal of Thermal Analysis and Calorimetry*, vol. 143, no. 2, pp. 1413–1424, 2021.

[51] M. Khan, A. Rasheed, T. Salahuddin, and S. Ali, "Chemically reactive flow of hyperbolic tangent fluid flow having thermal radiation and double stratification embedded in porous medium," *Ain Shams Engineering Journal*, vol. 12, no. 3, pp. 3209–3216, 2021.

[52] M. Khan and A. Rasheed, "Exothermic impact on Eyring-Powell nanofluid flow through a heated surface embedded in porous medium with thermal radiation: a numerical study," *Physica Scripta*, vol. 96, no. 3, Article ID 035213, 2021.

[53] A. Rasheed and A. Q. Khan, "Numerical simulation of fractional Maxwell fluid flow through Forchheimer medium," *International Communications in Heat and Mass Transfer*, vol. 119, Article ID 104872, 2020.

[54] M. S. Anwar, "Numerical study of transport phenomena in a nanofluid using fractional relaxation times in Buongiorno model," *Physica Scripta*, vol. 95, no. 3, Article ID 035211, 2020.

[55] T. Anwar, P. Kumam, and W. Watthayu, "An exact analysis of unsteady MHD free convection flow of some nanofluids with ramped wall velocity and ramped wall temperature accounting heat radiation and injection/consumption," *Scientific Reports*, vol. 10, no. 1, Article ID 17830, 2020.

[56] R. Sadiq, Q. M. Khan, A. Mobeen, and A. J. Hashmat, "*In vitro*toxicological assessment of iron oxide, aluminium oxide and copper nanoparticles in prokaryotic and eukaryotic cell types," *Drug and Chemical Toxicology*, vol. 38, pp. 152–161, 2015.